Microtubule-associated Protein 2c Reorganizes Both Microtubules and Microfilaments into Distinct Cytological Structures in an Actin-binding Protein-280–deficient Melanoma Cell Line

C. Casey Cunningham,* Nicole Leclerc,‡ Lisa A. Flanagan,* Mei Lu,‡ Paul A. Janmey,* and Kenneth S. Kosik‡

*Department of Medicine, Division of Experimental Medicine, ‡Department of Neurology, Center for Neurologic Diseases, Brigham and Women's Hospital and Harvard Medical School, Boston, Massachusetts 02115

Abstract. The emergence of processes from cells often involves interactions between microtubules and microfilaments. Interactions between these two cytoskeletal systems are particularly apparent in neuronal growth cones. The juvenile isoform of the neuronal microtubule-associated protein 2 (MAP2c) is present in growth cones, where we hypothesize it mediates interactions between microfilaments and microtubules. To approach this problem in vivo, we used the human melanoma cell, M2, which lacks actin-binding protein-280 (ABP-280) and forms membrane blebs, which are not seen in wild-type or ABP-transfected cells. The microinjection of tau or mature MAP2 rescued the blebbing phenotype; MAP2c not only caused cessation of blebbing but also induced the formation of two distinct cellular structures. These were actin-rich lamellae, which often included membrane ruffles, and microtubule-bearing processes. The lamellae collapsed after treatment with cytochalasin D, and the processes retracted after treatment with colchicine. MAP2c was immunocytochemically visualized in zones of the cell that were devoid of tubulin, such as regions within the lamellae and in association with membrane ruffles. In vitro rheometry confirmed that MAP2c is an efficient actin gelation protein capable of organizing actin filaments into an isotropic array at very low concentrations; tau and mature MAP2 do not share this rheologic property. These results suggest that MAP2c engages in functionally specific interactions not only with microtubules but also with microfilaments.

A nearly universal property of cells is their ability to change shape. Shape changes require the coordinate reorganization of the microtubule and microfilament cytoskeletal systems. The growth of neuronal processes, heralded by the presence of a growth cone at the advancing tip, represents an extreme degree of shape change over the course of development. Within growth cones, microtubules from more proximal central regions penetrate the dense peripheral actin meshwork to guide process advance (Tanaka and Sabry, 1995). Drugs such as colchicine or vinblastine applied at low concentration to suppress microtubule dynamics (Toso et al., 1993; Panda et al., 1995) can kinetically stabilize microtubules and impair process advance (Tanaka et al., 1995; Rochlin et al., 1996). These studies imply that microtubule penetration into the actin meshwork of the distal lamella depends upon the dynamic properties of microtubules and is required for process advance.

While the dynamic properties of microtubules may mediate their penetration into the actin meshwork, at the same time the dense isotropic organization of the actin filaments presents a barrier to the uncontrolled forward elongation of microtubules. An early demonstration of the restrictive role of F-actin was observed in the large Aplysia growth cones treated with cytochalasin (Forscher and Smith, 1988). After the loss of F-actin, microtubules extended into the lamellar region and often reached the peripheral margin. Similarly, microtubule-based process formation after treatment with cytochalasin is also seen in avian erythrocytes (Winkler and Solomon, 1991) and astroglial cells (Baorto et al., 1992). Although microtubule-microfilament interactions can be visualized in the growth cone, experimentally determining the molecular basis for these interactions is difficult in primary neurons. We used a nonneuronal cell with a cortical actin defect to determine the effects of specific microtubule-associated proteins (MAPs)[1] on microtubule and microfilament organization during the elaboration of a lamella and processes.

Address all correspondence to Kenneth S. Kosik, Center for Neurologic Diseases, Brigham and Women's Hospital, 221 Longwood Avenue-LMRC 112, Boston, MA 02115. Tel.: (617) 732-6460. Fax: (617) 732-7787.

1. *Abbreviations used in this paper*: ABP, actin-binding protein; CD, cytochalasin D; DIC, differential interference contrast; MAP, microtubule-associated protein; Sf9, Spodoptera frugiperda.

In this paradigm, microtubule-bearing processes emerge by penetrating a cortical actin bundle.

MAP2 is a heat-stable phosphoprotein that consists of a microtubule-binding domain at the carboxy terminus and a long projection domain within which a developmentally regulated splicing event (Garner and Matus, 1988) introduces 1,372 amino acids (Kindler et al., 1990; Papandrikopoulou et al., 1989). This splicing event shifts the apparent molecular mass of MAP2 on SDS-PAGE gels from a ~70-kD juvenile form (termed MAP2c) to a ~280-kD mature form. When MAP2c was transfected into hepatoma cells, Edson et al. (1993) showed processes were induced only after the cells were treated with cytochalasin. The result was interpreted to support a barrier function for the cortical actin gel, and the increased rigidity of the microtubules once bound to MAP2c were competent to penetrate the peripheral actin cytoskeleton only when it was disrupted by cytochalasin.

Other data have pointed to a more complex role for MAP2c in process emergence. Normally, cultured neurons elaborate a lamella-like structure around the entire periphery once attached to the dish, followed within hours by the consolidation of the lamella into a symmetric array of minor neurites. Suppression of MAP2 and MAP2c with antisense oligonucleotides results in the failure of the lamella to consolidate into minor neurites (Caceres et al., 1992), a function that requires a shift in the organization of the cytoskeleton from an actin-based lamella to a microtubule-based neurite. Consistent with this result was the induction of multiple minor processes when MAP2c was expressed in Sf9 cells (Leclerc et al., 1996). In comparison to other MAPs, these morphogenic features uniquely characterize MAP2c when it is either suppressed or expressed. For example, when the microtubule-associated protein, tau, was suppressed in neuronal cultures, the cells were competent to elaborate minor neurites but failed to selectively elongate one neurite and thereby generate an axon (Caceres and Kosik, 1990; Caceres et al., 1991). A comparable "gain-of-function" occurred when tau was expressed in Spodoptera frugiperda (Sf9) cells: the rapid elongation of a single process occurred (Baas et al., 1991; Knops et al., 1991).

Together these data allowed us to posit a role for MAP2c in early process formation at the interface between microtubules and microfilaments when cells convert their lamellae to a consolidated process. To investigate the relationship of MAP2c to these two filament systems, we used the M2 cell, one of three previously described cell lines derived from a malignant melanoma that lacked the major actin filament cross-linker, actin-binding protein (ABP, ABP-280) (Cunningham, C.C., H.R. Byers, J.H. Hartwig, T.P. Stossel, and D.J. Kwiatkowski. 1989. *J. Cell Biol.* 109: 277a). ABP-280 is important in the construction of the broad, ruffling lamellae seen in motile cells (for review see Stossel, 1993) because of its ability to construct a dense meshwork of highly branched actin filaments (Brotschi et al., 1978; Hartwig and Shevlin, 1986; Janmey et al., 1990). Cells from the ABP-280–deficient lines cannot quickly form a stable actin network and therefore display the characteristics of poor cortical actin gelation, including an absent peripheral clear zone, poor crawling behavior, and decreased membrane stability, as evidenced by extensive, prolonged membrane blebbing (see Fig. 1). All of these manifestations can be visibly corrected by the reexpression of ABP-280, either by transfection (Cunningham et al., 1992) or microinjection (unpublished results). These cells, which do not normally express any MAP2 isoform, provided the opportunity to observe the interactions of MAP2c not only with microtubules but also with actin devoid of its highly cross-linked structure, and thereby revealed additional organizational properties of MAP2c.

Materials and Methods

Reagents

All reagents were obtained from Sigma Chemical Co. (St. Louis, MO) unless otherwise specified. Colchicine was prepared as a 10 mM stock solution in ethanol and diluted to 50 μM final concentration in the culture media. Cytochalasin D was prepared as a 1 mM stock solution in ethanol and diluted to 2 μM in the media. Taxol was prepared as a 10 mM stock in ethanol, diluted to 1 μM in the media, and incubated with the cells for 20–30 min.

Cell Culture

The melanoma cell lines were cultured in minimal essential media (MEM) (GIBCO BRL, Gaithersburg, MD) supplemented with 10 mM Hepes, 8% newborn calf serum, and 2% FCS. Sf9 cells were obtained from American Type Culture Collection (ATCC No. CRL 1711; Rockville, MD) and were used to propagate wild-type and recombinant viruses. Sf9 cells were grown as a monolayer at 27°C in Grace's medium (GIBCO BRL) supplemented with 10% (vol/vol) FCS.

Videomicroscopy

Cells were plated on a 25-mm glass coverslip and placed in a Leiden incubation chamber (Medical Systems Corp., Greenvale, NY) kept at 37°C and in a 5% CO_2 atmosphere on the microscope stage by means of a temperature controller (model TC102; Medical Systems Corp.). Differential interference contrast (DIC) and phase contrast microscopy were performed on an inverted microscope (model Axiovert 405M; Carl Zeiss, Inc., Thornwood, NY) with variously a 40×, 0.9 NA Plan-neofluor, a 63×, 1.4 NA Planapochromatic, or a 100×, 1.4 NA Planapochromatic lens.

Protein Isolation

MAP2c, mature MAP2, and tau were purified from baculoviral expression constructs in Sf9 cells. The expression of these MAPs in Sf9 cells was described previously (Leclerc et al., 1996). Briefly, cDNAs corresponding to MAP2c, mature MAP2, or the three-repeat juvenile tau isoform were cloned into the transfer vector pVL1392 and then introduced into the genome of the baculovirus, *Autographa californica* multiple polyhedrosis virus (AcMNPV) by homologous recombination. The transfer vector was cotransfected with a modified form of AcMNPV, designated AcRP6-SC (Kitts et al., 1990), into Sf9 cells using the Lipofectin procedure (Gibco Laboratories, Grand Island, NY). After 48 h at 27°C, the infection supernatant was purified by a standard plaque-assay for occlusion body negative recombinant viral plaques by limiting dilution (Fung et al., 1988). The recombinant virus was amplified to yield titers of 10^8 to 10^9 plaque-forming U/ml. MAP2c, mature MAP2, and tau were purified from lysed infected cells by adjusting the low-speed supernatant to 0.75 M NaCl, boiling for 5 min, and centrifuging at 200,000 *g* for 30 min. After precipitation with ammonium sulfate, the proteins were collected by low-speed centrifugation, resuspended in 1.2 M KI buffer (1.2 M KI, 1 mM EGTA, 10 mM imidazole, 0.5 mM DTT, pH 7.4), and then collected again by a low-speed centrifugation. After purification, the proteins were dialyzed extensively against injection buffer (120 mM KCl, 10 mM KH_2PO_4, pH 7.2), concentrated to between 1 and 3.5 mg/ml, aliquotted and frozen at −80°C before use. Some mature MAP2 preparations included the protease inhibitor diisopropyl fluorophosphate, and some was obtained commercially from bovine brain (Cytoskeleton, Denver, CO). None of these modifications altered any of the results.

Microinjection

Microinjection was performed on the inverted microscope equipped with a Narishige micromanipulator and pneumatic injector (Narishige USA, Inc., Greenvale, NY). Needles were pulled on a vertical needle puller and beveled as needed on a rotating grinder (both from Narishige USA, Inc.). All injections were performed with the cells kept at 37°C and in a 5% CO_2 atmosphere. Injection volumes were estimated at <20% of total cell volume both by comparing cell images during injection and based on subsequent cell viability, as previous studies suggest that cells do not survive with injection volumes >15% of total cell volume (Cooper et al., 1987). A series of control injections was performed with injection buffer alone in varying volumes for all experiments. Since, with time, M2 cells slowly establish a peripheral gel from actin filament interpenetration alone (Cunningham, 1995), all injections were performed in cells less than 36 h after plating. Each result reported is based on injections of at least 50 cells, unless otherwise noted.

Antibodies and Indirect Immunofluorescence Microscopy

For immunofluorescence, cells were fixed for 15 min at room temperature in 3.7% paraformaldehyde in PBS and 0.12 M sucrose. They were then washed in PBS and permeabilized in either 0.3 or 0.5% Triton X-100 for 5 min. For some experiments, cells were simultaneously fixed and extracted for 10 min in fixative plus 0.1% saponin and 250 nM FITC-phalloidin (Sigma Chemical Co.), and 10 mM EGTA to stabilize actin filaments. After blocking of nonspecific binding sites with 5% BSA in PBS, the cells were incubated first with the specific primary antibody overnight at 4°C, then with secondary antibody at 50 μg/ml of either rhodamine or fluorescein-conjugated goat anti–mouse IgG (Cappel Labs, Durham, NC) or donkey anti–rat IgG (Jackson Laboratories, Bar Harbor, ME) for 2 h at room temperature, and then washed in PBS with 0.2% gelatin in between. For actin staining, fluorescein or rhodamine-labeled phalloidin (Sigma Chemical Co.) was added at 250 ng/ml to the secondary antibody incubation. Antibodies used were AP18 against MAP2c (Binder et al., 1986), and YL1/2 rat monoclonal against tubulin (Accurate Chemical and Scientific, Westbury, NY). The cells were viewed on a microscope (model Axioplan 405M; Carl Zeiss, Inc.) equipped for epifluorescence or an inverted microscope (model Diaphot-TMD; Nikon, Inc., Melville, NY). Images were analyzed with the Image I software program (Universal Imaging Corp., West Chester, PA) and processed in Adobe Photoshop (Adobe Systems Inc., Mountain View, CA) to maximize signal to noise ratios.

Rheometry

The effects of each MAP on the viscosity of a solution of actin filaments were compared by falling ball viscometry (Pollard, 1982), and the viscoelastic properties of actin gels were measured by dynamic oscillatory methods (Janmey, 1991). In the falling ball assay, 0.5 mg/ml actin was mixed with 1:1,500 gelsolin and varying concentrations of the candidate cross-linking protein. After addition of salts to initiate polymerization, the mixture was drawn into a 100 μl capacity glass capillary tube and allowed to polymerize for 2 h. The tubes were then slanted to a 45° angle, and the time required for a 0.025-inch stainless steel ball to travel the length of the tube was measured. The measurements are presented as relative viscosity compared to actin filaments polymerized without cross-linker.

The dynamic shear viscoelastic properties were measured using a torsion pendulum. Measurements were performed in a buffer at pH 7.4 consisting of 2 mM $MgCl_2$, 150 mM KCl, 0.2 mM $CaCl_2$, 0.2 mM DTT, 0.5 mM ATP, and 0.3 mM Pi. The storage modulus was calculated from the frequency of free oscillations ranging between 0.1 and 10 Hz for 1.6 mg/ml actin polymerized in the presence of gelsolin (1:200) and ABP-280 (1:133) or MAP2c (1:100) as previously described (Janmey, 1991). Viscoelasticity was also measured in collaboration with Soren Hvidt (Roskilde, Denmark) using a Rheometrics (Piscataway, NJ) RFS instrument operating in a forced oscillation mode, as previously described (Janmey et al., 1988).

Bundle formation was measured by dynamic light scattering using a Brookhaven Instruments BI30AT apparatus (Holtsville, NY) with a 128-channel autocorrelator and a 10 mW He-Ne laser emitting 633-nm light. Actin (3 μM) was polymerized for 4 h with various concentrations of MAP2c in siliconized glass tubes (6-mm inner diameter). The total scattering intensity and the autocorrelation function of quasielastically scattered light were determined by standard methods (Hartwig et al., 1992). An increase in polymer mass/length ratio would retard the decay of the autocorrelation function and increase the total scattering intensity if MAP2c caused lateral association of actin filaments. This method has been used previously to document the bundling activity of tensin (Lo et al., 1994) and myristoylated alanine-rich C kinase substrate (Hartwig et al., 1992).

Results

Microinjection of MAP2c into M2 Cells Leads to Cortical Gelation and Process Formation

M2 cells lack ABP, and when freshly plated, they appear rounded or polygonal in shape, do not form lamellae, are unable to constrain intracellular organelles from their periphery, and display prolonged, extensive membrane blebbing from the entire cell perimeter (Fig. 1 *A*). Transfection of the ABP cDNA into this line completely corrects these defects (Fig. 1 *B*). Within 5 min after injection of 50 μM MAP2c (maximum estimated final intracellular concentration is 5 μM), the M2 cells stopped membrane blebbing and formed a flattened peripheral lamella (Fig. 2). In some cells, several separate lamellae developed, while in other cells the peripheral flattening was circumferential. Consistent with the identity of these peripheral structures as lamellae, intracellular organelles (which average ~1 μm in diameter in these cells) were excluded.

In most of the cells injected (75%), multiple, long processes (average 40 ± 12 per cell) emerged from the lamellar margin 10–20 min after MAP2c microinjection. By phase contrast microscopy long, rigid, spikelike structures that probably represented microtubule bundles traversed the processes and originated well within the cell interior. In some cells, these processes formed a radial array around the entire cell circumference. Time-lapse videomicroscopy revealed that in all cases process formation began after the elaboration of the lamella. Ruffling of the cell edge was frequently observed, and often preceded process formation (Fig. 3). However, once process formation occurred, no further ruffling was observed in those areas, although some cells displayed separate areas of continued ruffling.

The morphologic effects of MAP2c were concentration dependent. Microinjection of 25 μM MAP2c within the micropipette gave similar results to those above, except that only 50% of the cells developed processes. At 12 μM MAP2c within the micropipette, there was less peripheral clearing, only 30% of the cells had processes, and the number of processes per cell decreased to an average of 15. 6 μM MAP2c did not induce lamellae or processes. Every concentration, including 6 μM, did cause the cessation of blebbing. Therefore, although some of the morphologic effects may require MAP2c in excess of physiological concentrations, exceedingly low concentrations rescue the blebbing phenotype.

Control injections with either injection buffer alone or with purified supernatant from Sf9 cells infected with the wild-type virus did not induce any morphologic changes in the cells. Taxol (1 μM), which stabilizes microtubules and thus promotes their polymerization, also did not lead to process formation or lamellar formation in these cells. Additional controls used the A4, A6, and A7 clonal sublines created from the transfection of the cDNA for ABP-280 into cells from the ABP-deficient line M2. The three lines differ in their expression of ABP-280 with A6 expressing

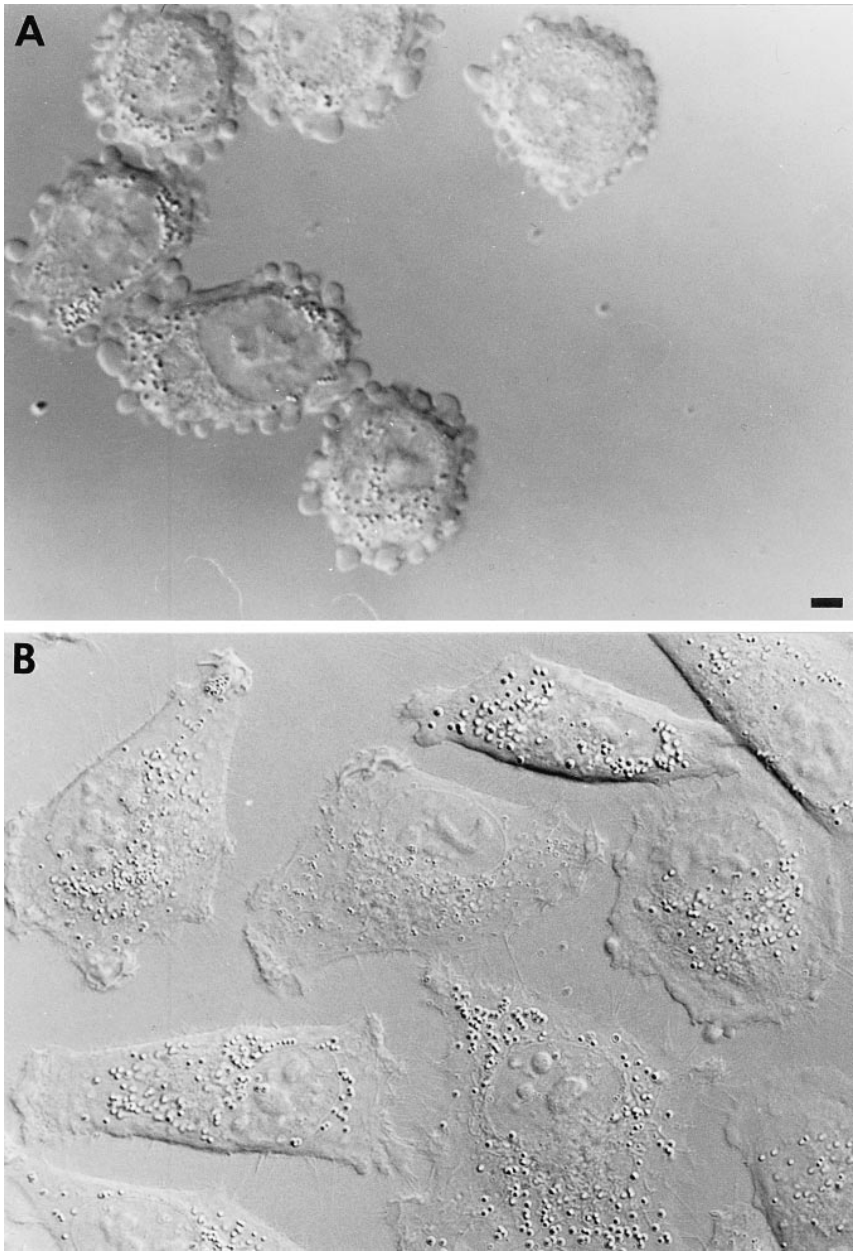

Figure 1. Differential interference contrast (DIC) photomicrograph of (*A*) ABP-280–deficient M2 cells with profuse membrane blebs and (*B*) the A7 clonal subline created by transfecting the cDNA for ABP-280 into cells from the ABP-deficient line, M2. Bar, 5 μm.

much less than the other two (Cunningham et al., 1992). In contrast to the morphology of the M2 cells, cells from all three transfected lines have a peripheral lamella and increased cortical viscosity by rheological measurements. Consistent with the low ABP-280 in the A6 cells, these cells also have a lower cortical viscosity (Cunningham et al., 1992). Injection of 50 μM MAP2c into A6 cells resulted in process formation in 50% of the injected cells (24 out of 50) and an average of 11 processes per cell. Injection of cells from A4 or A7 cell lines induced processes in only 2 of 102 (<2%) cells. None of the injections caused an enlargement of the lamella. These observations suggested a negative correlation between the ability of MAP2c to form processes and the levels of ABP-280 in cells.

MAP2c Is Present in Regions Devoid of Tubulin

Having observed two distinct cytological structures—lamellae and processes—we sought to determine whether MAP2c was present in both of them. Indirect immunofluorescence with antibodies to MAP2c revealed diffuse labeling that ranged from faint to moderate intensity within the cell body and the lamellae. Focal regions of the cell, such as ruffles (Fig. 4 *B*) and processes (Fig. 4 *E*), often contained more intense MAP2c immunoreactivity. It was clear that microinjected MAP2c was not uniformly distributed throughout the cytoplasm.

Some regions of the cell where MAP2c label was observed are known to be highly enriched in actin filaments and have a relative paucity of microtubules. We searched for cellular regions where MAP2c was likely to be present in the absence of microtubules. The membrane ruffle is such a region that is known to lack microtubules. The identification of the ruffle was confirmed by staining with FITC-phalloidin, and colocalization of MAP2c to the same site was observed by double labeling with a MAP2c anti-

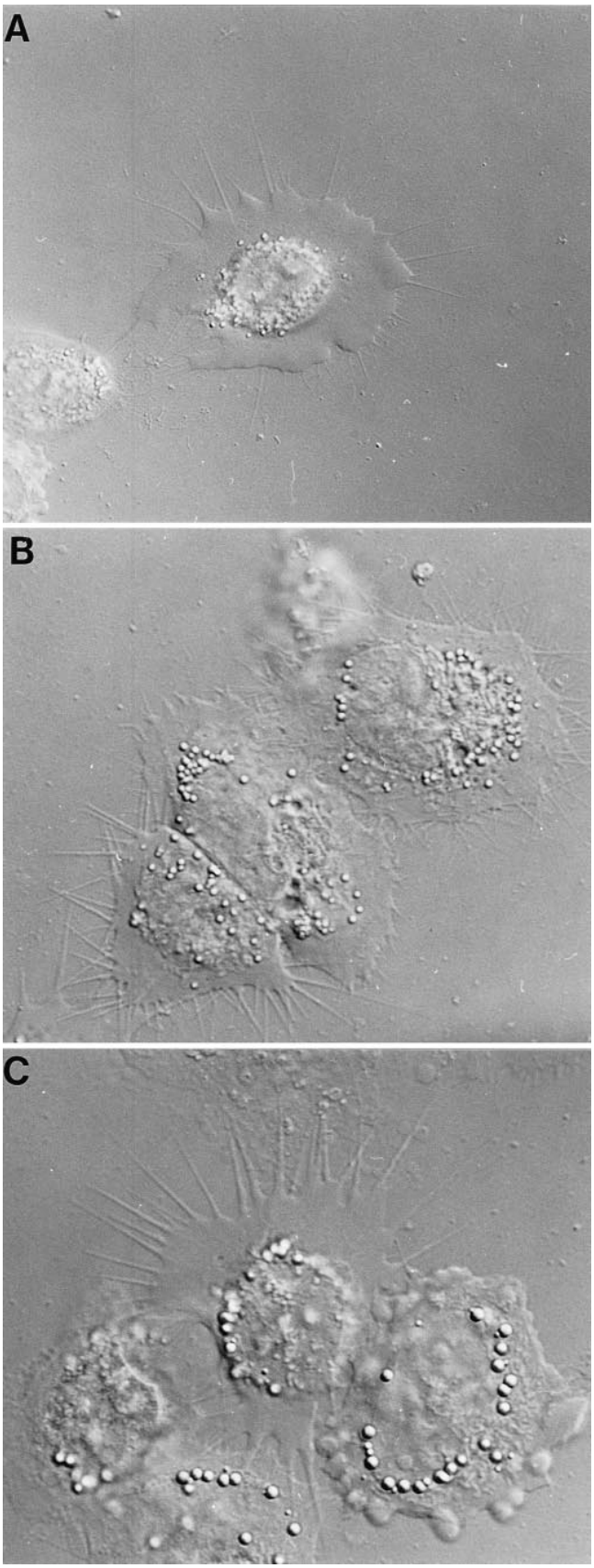

body (Fig. 4, *A–C*). An association of MAP2c with the cytoskeleton was indicated by the retention of staining after detergent extraction at the time of fixation. The presence of MAP2c in a membrane ruffle strongly points to the presence of this molecule in an actin-rich region known to lack microtubules. Tubulin antibodies demonstrated that microtubules often course through lamellae, but there are sites within lamellae that lack microtubules. Although all lamellae reacted with MAP2c antibodies above background levels, regions of the lamellae that lacked staining with tubulin antibodies remained reactive with MAP2c antibodies (Fig. 4, *D–F*). This observation suggested that MAP2c was present in regions of the lamellae that lacked tubulin, but contained actin filaments.

Microinjection of Mature MAP2 and Tau Protein Have More Limited Effects on Cell Shape than MAP2c

In contrast to MAP2c, the microinjection of the mature isoform of MAP2 did not usually induce either a lamella or processes. All concentrations of mature MAP2 up to 50 μM within the micropipette induced the cessation of blebbing in M2 cells. In 30 of 35 cells injected (85%), no processes formed after MAP2 injections; in the remaining cells, 1–3 processes formed and rarely was there a small lamella (Fig. 5 *A*). These processes were wider and more tapered than those observed in the MAP2c-injected cells, and by phase microscopy, the thickened bundles within their processes did not extend very far into the cell body. A similar inhibition of blebbing was seen with injections of decreasing MAP2 concentrations down to 6 μM, at which point there was no detectable effect on 36 out of 36 injected cells.

Likewise, injections of three repeat tau (50 μM in the micropipette) did not lead to cortical gelation with lamella or process formation in 47 of 60 cells. However, in contrast to vehicle injections and like mature MAP2, tau did result in the complete cessation of blebbing (Fig. 5 *B*). Two cells elaborated three to five short uniform processes that contained thickened bundles of microtubules that originated within the cell body by phase contrast microscopy. Injections of more dilute tau did not change the cellular morphology.

Differential Vulnerability of MAP2c-induced Cytological Structures to Depolymerizing Drugs

Evidence that the MAP2c-induced processes were microtubule based was derived from treatment of the cells with colchicine (Fig. 6 *B*). M2 cells microinjected with MAP2c and then incubated with colchicine at 50 μM final concentration showed a decrease or disappearance of processes in 27 of 30 process-bearing cells (90%), within 20 min. Thus, most of the microtubules within the processes were sensitive to colchicine. However, after colchicine treatment the MAP2c-induced lamella remained nearly intact. In 17 cells, there was a slight decrease (at most 25%) in the

Figure 2. DIC photomicrographs of M2 cells 20 min after microinjection with 50 μM MAP2c. (*A*) The microinjected cell in the center demonstrates both the lamella and array of processes. (*B*) Three microinjected cells with a range of lamellar morphologies. (*C*) A microinjected cell adjacent to a noninjected cell.

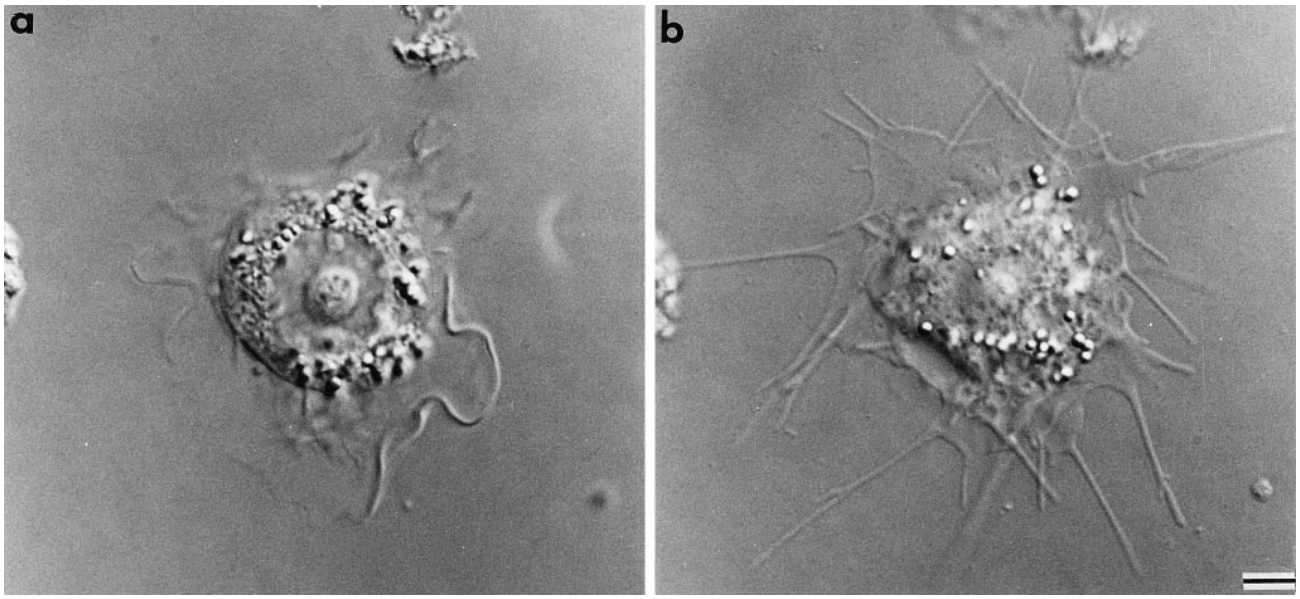

Figure 3. DIC photomicrographs showing the progression of morphologic changes in an M2 cell microinjected with 50 μM MAP2c. (*a*) 5 min after injection, the cell displays a broad, ruffling lamella. (*b*) 20 min after injection, ruffling has ceased and process formation has begun. Bar, 5 μm.

width of the peripheral lamellae. To determine whether microtubule polymerization was initially required to form the peripheral lamellae, cells were preincubated with 50 μM colchicine and then injected with MAP2c (Fig. 6 *C*). Of 26 viable cells remaining after injection, lamellae developed in 18 (70%), but processes did not form in any cell. This result suggested that after MAP2c microinjection, lamellae could form independently of the microtubules.

To assess the cytoskeletal systems involved in supporting MAP2c-induced lamellae, the M2 cells were treated with 3–5 μM cytochalasin D (CD), which inhibits barbed-end actin polymerization (Fig. 6 *A*). 25 μM MAP2c was loaded into the micropipette and injected; 20 min later, when the cells had ceased blebbing and developed a cortical veil, we added 3–5 μM CD to the medium. Of 83 cells so treated, 72 (86%) had a marked decrease in their lamellae (average reduction in width of cleared zone: 80 ± 20%) after 10–20 min of treatment with cytochalasin. Although there was a nearly complete collapse of the lamellae in many cells, the growth of the processes was actually enhanced. In 58 cells (70%), the average number of processes per cell doubled in number from 40 (± 12) to 85 (± 14). Furthermore, the average length of the processes increased from 27 μm (± 5) to 61 μm (± 15) in these cells. A similar experiment in A7 ABP-280–expressing cells also resulted in extensive process formation in nearly all injected cells (data not shown).

We next questioned whether intact microfilaments were required to initiate process formation by treating M2 with 3–5 μM CD for 10 min before they were microinjected with MAP2c. Under these conditions neither lamellae nor processes formed. These results raised the possibility that a focal site of "weakness" or loss of microfilament integrity in the cortical actin skeleton is required to initiate directed microtubule growth, rather than a complete depolymerization of the F-actin.

MAP2c Rearranges Both Microtubules and Actin Filaments in M2 Cells

Microinjection of MAP2c into M2 cells induces a reorganization of F-actin. In control noninjected or vehicle-injected cells, F-actin as detected with rhodamine-labeled phalloidin forms a submembranous rim (Fig. 7 *A*). Indeed, M2 cells do have a subcortical F-actin skeletal system; but in contrast to A7 cells, which contain ABP-280, M2 cells have a decrease in highly cross-linked actin (Cunningham, 1995). Injection of the M2 cells with MAP2c results in the loss of the cortical F-actin rim and a more diffuse labeling of the cells with rhodamine-phalloidin (Fig. 7 *B*). Much of the diffuse label corresponds to the broad lamellae induced by MAP2c.

Not surprisingly, MAP2c injection also induces a reorganization of the microtubules in a manner that has been re-

Figure 4. Exogenous MAP2c is present at sites devoid of tubulin but rich in actin. M2 cells, which normally lack all MAP2 isoforms, were microinjected with MAP2c. After MAP2c microinjection, the M2 cell with the three arrows was simultaneously fixed and extracted as described in Materials and Methods and visualized 5–10 min later by double labeling with FITC-phalloidin (*A*), MAP2c antibody, AP18 (*B*), and Nomarski optics (*C*). The arrows indicate a region of membrane ruffling in which F-actin and MAP2c colocalize. An MAP2c-injected cell was fixed and visualized by double labeling with tubulin antibody (*D*), MAP2c antibody, AP18 (*E*), and a Nomarski image (*F*). The arrow indicates a MAP2c-immunoreactive region of the cell that is devoid of tubulin staining and appears flattened. Bar, 10 μm.

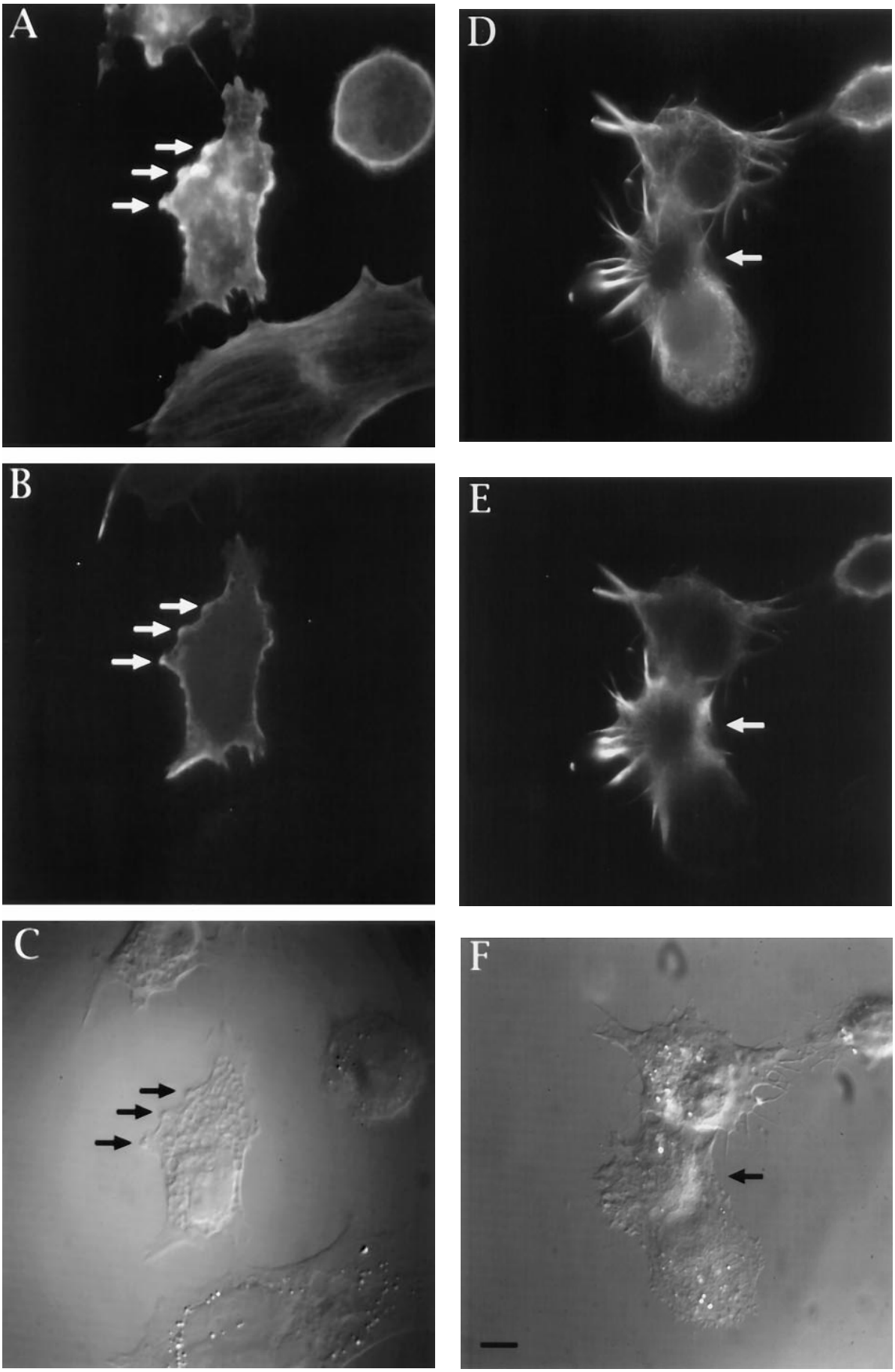
A
B
C
D
E
F

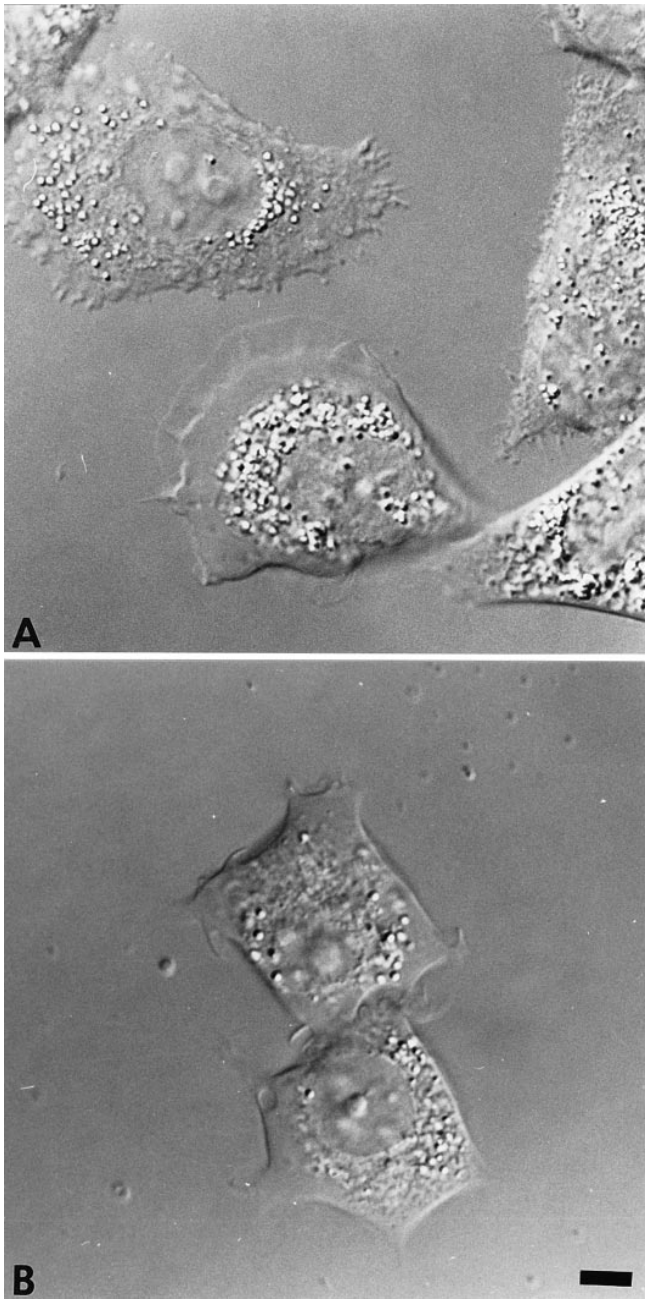

Figure 5. (*A*) M2 cells 20 min after microinjection with mature MAP2. All of the cells in the field were microinjected. One cell elaborated a small lamella. (*B*) M2 cells 20 min after microinjection with the three-repeat isoform of the tau protein. Both cells were microinjected. Bar, 5 μm.

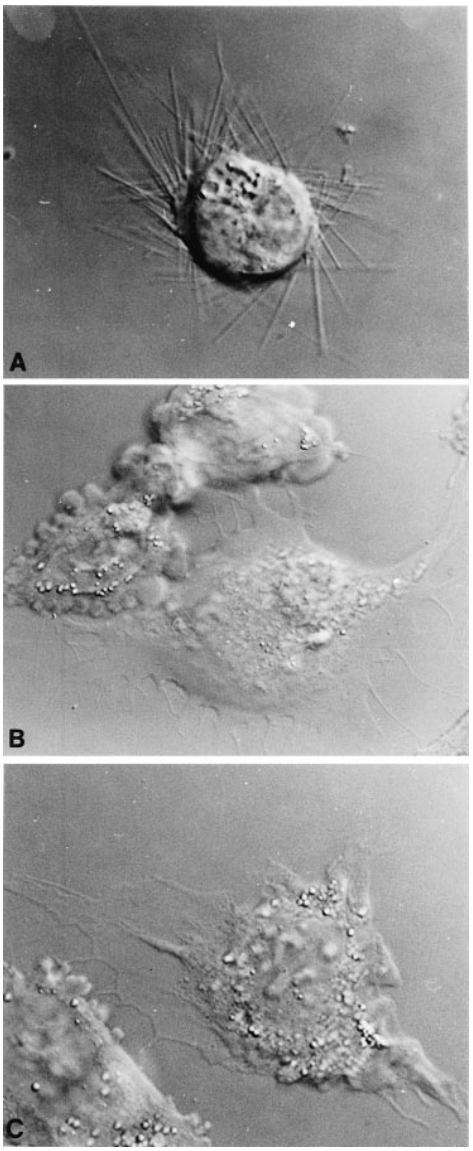

Figure 6. Effects of colchicine and cytochalasin administration on MAP2c-injected M2 cells. (*A*) MAP2c-injected M2 cell incubated with 2 μM cytochalasin D leading to collapse of the peripheral lamella and an enhancement of process formation. (*B*) Treatment of MAP2c-injected M2 cells with 50 μM colchicine leads to loss of processes but retention of the lamella. (*C*) An M2 cell preincubated with colchicine and then injected with MAP2c displays lamellar formation but fails to elaborate processes.

ported previously (Umeyama et al., 1993). For 24 h after plating, M2 cells have few discernible microtubules, and as they spread further they develop a dispersed microtubule network. However, the injection of MAP2c induces large bundles of microtubules in the cell body and processes. Microtubule bundles within processes often appear to originate deep within the cell body. Microtubules sometimes extend in a more dispersed pattern into the lamella. Particularly, in cells that do not form processes, bundled microtubules loop around the perimeter of the cell. When MAP2c was injected into A7 cells, similar microtubule bundles formed, but as noted above, the cells did not form processes.

MAP2c Causes Actin Gelation In Vitro

Because the morphologic changes induced by MAP2c in the M2 cells imply effects on the cortical actin network, we measured the ability of the protein to increase the viscosity of a dilute solution of actin filaments in vitro. Such solutions of short polymers are usually fluid, but if some of the polymers are either increased in length or tied together by a cross-linking protein, the decrease in overall free rotational motion of the filaments results in an in-

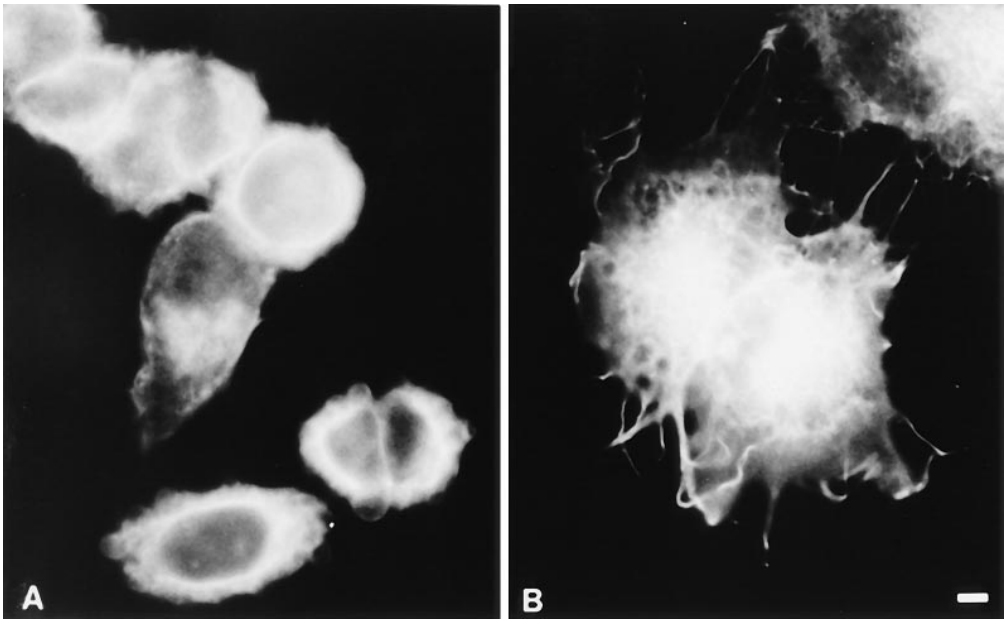

Figure 7. Freshly plated M2 cells stained for F-actin by rhodamine-labeled phalloidin. (*A*) Uninjected cells constrain F-actin within the cortical rim. (*B*) Cells 20 min after injection with 25 μM MAP2c show F-actin in a more diffuse pattern corresponding to the newly elaborated lamella. Bar, 5 μm.

creased viscosity of the total solution. This increase is most dramatic in solutions where most of the filaments are effectively immobilized, resulting in a phase transition to a gel-like state (Flory, 1953).

Increases in actin viscosity due to the effects of a candidate cross-linking protein can be quantitated in several ways. One method is to measure the differences in the impedance presented to a small ball moving through the solution, as measured by the amount of time required for the ball to move a preset distance, in a falling ball viscometer (Pollard, 1982). If the length of the actin filaments in a solution of standard actin concentration is kept constant, various candidate cross-linking proteins can then be compared by the amount of each required to achieve a certain viscosity, or to cause gelation. If the affinity of the candidate protein for actin filaments is uniformly high, then the efficiency of each protein in producing gelation depends upon the geometry of the filaments allowed by the cross-linker (Flory, 1953; Almdal et al., 1993). In mammalian

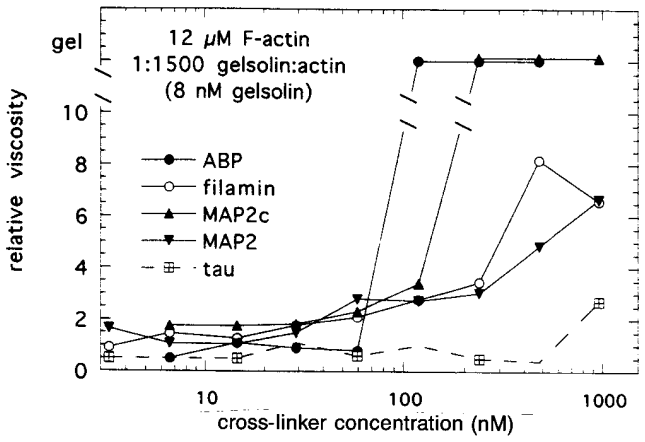

Figure 8. Cross-linking of actin filaments in a falling ball viscometer by MAP2c, MAP2, and tau compared to ABP-280 and its related isoform filamin.

cells, the most efficient gelation protein is ABP-280 because of its ability to form near right-angle cross-links between filaments (Janmey et al., 1990).

We measured the ability of each of the MAPs to increase the viscosity of, or to gel, a solution of short actin filaments in a falling ball viscometer. Actin filaments polymerized in the presence of MAP2c reached a gel state at concentrations similar to those at which ABP-280 gels actin (Fig. 8). In contrast, tau and mature MAP2 were unable to gel the same concentration of actin filaments at these or any other molar ratios tested, although they did increase viscosity. Mature MAP2 was superior to tau in increasing the viscosity of actin filaments.

Similar results were obtained by measuring the elastic shear moduli of solutions of actin filaments polymerized in the presence of each protein in a torsion pendulum (Janmey, 1991). The elastic shear modulus is a measure of a solution's resistance to shear stress, and actin gels formed by MAP2c/actin mixtures had a greatly increased elastic shear modulus (Fig. 9). In contrast, tau at equivalent molar ratios to actin resulted in a much lower increase in the elastic shear modulus of an F-actin solution. The increase seen with MAP2c was dose dependent with MAP2c concentration (Fig. 9 *A*) and was not due to greater filament length, as MAP2c did not affect the kinetics or extent of actin polymerization as judged by pyrene-labeled actin assembly (data not shown).

To determine if the initial increases in elastic shear moduli seen with MAP2c could be due solely to bundling of actin filaments, we then measured the relative light scatter of solutions of actin filaments with and without varying concentrations of MAP2c. At dilute molar ratios of MAP2c to actin, where an increase in the elastic shear modulus was already apparent, there was no increase in relative light scatter. Higher molar ratios of 1:86 increased the light scattering (Fig. 9 *A*, *inset*). These results suggest that dilute concentrations of MAP2c caused actin gelation by organizing the actin filaments into an isotropic network; only at higher molar ratios or lower ionic strength (data not

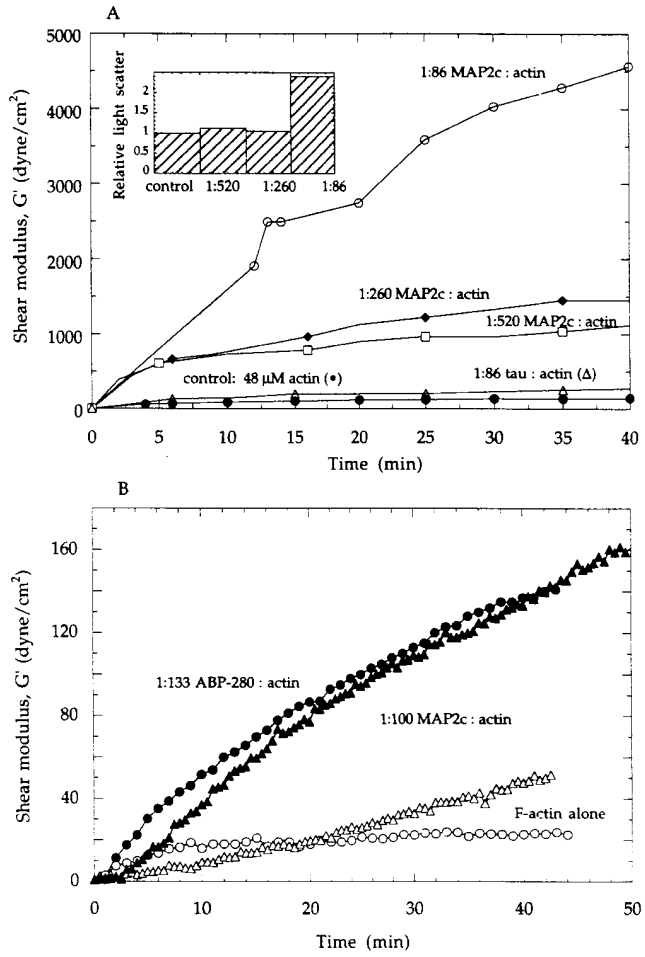

Figure 9. Effect of MAP2c on the shear elastic modulus of actin gels. (*A*) MAP2c at low molar ratios before actin polymerization greatly increases the shear elastic modulus of the resultant actin gel but without a significant increase in light scattering, implying that the gel is due to high-angle cross-linking. (*B*) Short actin filaments produced by a gelsolin (8 nM)/F-actin (12 μM) mixture are cross-linked with similar efficiency by MAP2c and ABP-280. Open characters are matched controls for closed characters.

shown) do actin bundles form. Because this behavior is similar to ABP-280, we directly compared their effects on actin. The shear moduli of networks composed of short actin filaments cross-linked by either MAP2c or ABP-280 (Fig. 9 *B*) showed that similar molar ratios of MAP2c and ABP-280 (corresponding to a smaller weight ratio for MAP2c) produced actin networks of very similar shear moduli, and both were much greater than those of the corresponding actin solutions without cross-links.

Discussion

In Vitro Behavior of MAP2c Predicts Its Effects on M2 Cells

Process emergence involves an exquisitely controlled coordination between two cellular structures: an actin-rich lamella and a microtubule-rich shaft. The consolidation of the lamella into a shaft requires interactions between microtubules and microfilaments. The studies described here support the hypothesis that MAP2c can serve as a mediator between the actin filaments and the microtubules because it can engage in functional interactions with both systems. Other studies have described in vitro interactions between MAPs and actin, and some of these have identified the microtubule-binding domain within the MAP as the approximate binding site (Griffith and Pollard, 1978, 1982; Nishida et al., 1981; Satillaro et al., 1981; Pollard et al., 1984; Asai et al., 1985; Satillaro, 1986; Correas et al., 1990; Dentler and Adams, 1992; Cross et al., 1993; Moraga et al., 1993). All of these studies predate the discovery of MAP2c. A few studies have noted other proteins that may link microtubules and actin filaments, including ezrin (Birgbauer et al., 1991), calcineurin (Ferreira et al., 1993), and $p150^{glued}$ (Waterman-Storer et al., 1995).

The in vitro data here show that the interaction of MAP2c with actin filaments differs from tau and mature MAP2 in that binding at low concentration results in the formation of an isotropic actin network rather than actin bundles (Fig. 9). The lack of a significant increase in light scatter in the presence of low molar amounts of MAP2c indicates that the large increase in elastic modulus at these concentrations cannot be attributed to lateral associations between actin filaments resulting in bundles, as was previously proposed for MAP2 (Pollard et al., 1984; Satillaro et al., 1981). More likely, the gel formed by MAP2c is due to an isotropic network of filaments branching at high angles (Flory, 1953). The smaller increases in viscosity and elastic shear moduli seen with tau and mature MAP2 are more likely due to their actin-bundling ability. In fact, MAP2c and tau show comparable increases in light scattering (data not shown), which also suggests that at concentrations of MAP2c above those required to induce actin filament isotropy, MAP2c, like tau, bundles actin filaments. MAP2c is unique in its ability to induce an isotropic network of actin filaments at concentrations below those required for mature MAP2 or tau, or even MAP2c itself, to bundle actin filaments.

Studies of chymotryptically digested fragments indicate that the actin-binding domain of MAP2c and MAP2 approximates the tubulin-binding domain (Satillaro, 1986), and a synthetic peptide corresponding to one of the repeated tubulin-binding sites in both MAP2 and tau also binds actin (Correas et al., 1990). Therefore, for actin filament cross-linking to occur, either multiple actin-binding domains exist (Selden and Pollard, 1986) or dimerization of the MAP2c molecule must occur. That MAPs can set microtubule–microtubule spacing (Chen et al., 1992; Leclerc et al., 1996) raises the possibility of dimer formation. Dynamic light scattering assays on pure preparations of MAP2c suggest the existence of oligomerized forms (Janmey, P.A., unpublished observations). Dimerization of tau and MAP2 isoforms has been reported (Wille et al., 1992*a*, *b*), and both form antiparallel dimers arranged so that the binding domains would be separated by the overlap length of the dimer (Wille et al., 1992*a*,*b*). These overlap lengths would clearly differ between MAP2c and mature MAP2.

In addition to different overlap lengths, other conformational properties of MAP2 versus MAP2c may account for their differential organizational properties in both in vitro and in vivo assays. In neurons as well as in other eukaryotic cells, MAP2 becomes highly phosphorylated. All of

the MAPs in these studies were synthesized and purified from Sf9 cells, which appear to phosphorylate MAP substrates similarly to the in vivo pattern. Nevertheless, significant phosphorylation differences may occur between mature MAP2 and MAP2c. A comparison of the primary structures of MAP2 and MAP2c with other known actin-binding proteins reveals little homology. However, a similar lack of homology is found among actin-binding domains in other proteins such as gelsolin and α-actinin (Way et al., 1992). The binding of these proteins to F-actin relies on the formation of specific folds that interact with grooves in the actin filament (McLaughlin and Weeds, 1995). MAP2 and MAP2c may bind via similar mechanisms with differences in the spacing of their charge distributions accounting for the differences in actin gelation ability between the two isoforms.

Like MAP2c, tau and mature MAP2 rescue the blebbing phenotype and induce microtubule bundles in M2 cells; but unlike MAP2c, tau and mature MAP2 fail to induce either lamellae or processes. The M2 cell phenotype arises from a defect in actin cross-linking because of the absence of ABP-280. This defect in the cortical actin cytoskeleton gives rise to membrane blebs because there is decreased impedance to internal solvent flow, resulting in rapid expansions of the plasma membrane that outpace the usually stabilizing local actin polymerization (Cunningham, 1995). Proteins that increase the viscosity of the peripheral actin network decrease this solvent flow and reduce blebbing because of an accelerated formation of a peripheral actin gel. It therefore seems likely that all of the MAPs studied here are competent to increase the viscosity of the peripheral actin network. In contrast to MAP2c, the interaction of tau and mature MAP2 with actin in vitro induces bundle formation rather than the high angle cross-links of an isotropic network. This difference may account for the failure of tau and mature MAP2 to induce lamellae in M2 cells.

All of the MAPs studied here bundle microtubules when they are expressed in cells, including M2 cells. Why then do tau and mature MAP2 fail to induce processes in the M2 cells? Likewise, the treatment of M2 cells with taxol, which bundles microtubules, does not lead to process formation. Clearly, polymerization and bundling of microtubules alone is insufficient for process formation. To some extent process formation depends on the cell type—all of the tau and MAP2 isoforms are competent to form processes in Sf9 cells—whereas in fibroblasts and M2 cells they induce microtubule bundles, but not processes. What then are the critical components that lead from microtubule polymerization to the elaboration of processes? And why should MAP2c, which has a microtubule-binding domain that is identical to mature MAP2 and highly homologous to tau, be especially competent to initiate process outgrowth in M2 cells? The organization of the subcortical actin cytoskeleton and the specific molecules competent to interact with this filamentous system may represent the critical component for successful process outgrowth and account for the specificity of interacting molecules.

In Vivo Functions of MAP2c

In the M2 cells, MAP2c appears to have the expected property of cross-linking microtubules in the induced processes and the unexpected property of cross-linking actin filaments in ruffles and lamellae. These data suggest that MAP2c can form microfilament–microfilament cross-links and microtubule–microtubule cross-links; our data cannot address the question of whether microtubule–microfilament cross-links also occur. How might this dual cross-linking property serve in process elaboration? Penetration of microtubules into an organized actin framework, such as that of the growth cone, is required for process initiation and growth. Process emergence appears to involve the capture of several microtubules at a discrete site near the membrane, the bundling of these microtubules proximally where they funnel into the process shaft, and the deformation of the cell boundary as an incipient or elongating process.

One of the early requirements for process formation is the establishment of a microtubule orientation which directs elongation orthogonal to the cell perimeter. Actin filaments may contribute to establishing the correct microtubule orientation. When the margin of a cell consists of actin bundles, rather than an isotropic actin organization characteristic of a lamella, elongating microtubules often have a tendency to loop around the cell perimeter without penetrating the bundles or forming a process. This pattern is observed in the marginal band of dogfish red cells (Sanchez and Cohen, 1994) and sometimes in cells expressing MAP2c (Edson et al., 1993; Leclerc et al., 1996). In contrast, microtubules involved in process formation do not show this radial organization; their direction of elongation is orthogonal to the cell perimeter. Some degree of actin organization may be required to engage sufficient numbers of microtubule plus ends at a single site near the membrane to initiate a process. Support for this step in process formation is the observation here that M2 cells treated with cytochalasin before MAP2c injection failed to elaborate processes. F-actin may capture microtubules at a discrete and possibly specific site on the subcortical membrane, and once assuming a radial direction of elongation, efficient microtubule growth proceeds more efficiently with less resistance from an organized actin barrier. Evidence for the concomitant focal organization of actin at the initiation site of a process comes from observations of processes induced by tau expression in Sf9 cells (Knowles et al., 1994).

Once microtubule growth is directed approximately orthogonal to the membrane, the actin polymerization state appears capable of controlling microtubule elongation (Lin and Forscher, 1993). In the A4 and A7 cells there is sufficient ABP-280 to form actin cross-links and prevent MAP2c-induced processes. The lack of ABP-280 in the M2 cells and concomitant decrease in actin cross-linking may allow access for MAP2c–actin interactions. Once initiated, microtubule elongation is most efficiently translated into process elongation when there is minimal actin resistance. In this manner the cortical actin cytoskeleton serves not only as a barrier over most of the cell perimeter but also as a gate at sites of process emergence. Biochemical and mutagenesis studies with particular attention to the phosphorylation states of MAP2c will be required to determine whether this molecule can serve as a switch to mediate functionally distinct interactions between microfilament populations and microtubule populations leading to coordinate regulation of these two cytoskeletal systems.

Extracellular signals that affect local actin organization may also determine the specific site and orientation for microtubule growth. Regulated interactions between actin filaments and MAP2c may determine whether MAP2c will engage the cortical actin cytoskeleton in a manner that allows lamellar formation and penetration of microtubules through the actin meshwork. As observed in Aplysia growth cone, contacts induce a focal F-actin assembly that, in turn, guides microtubule redistribution to a target site (Lin and Forscher, 1993). Actin organization is responsive to extracellular signals via such intracellular messengers as phosphatidylinositol 4,5-bisphosphate and the small G proteins, rac and rho; however, the mechanism of signal transduction to microtubules is unknown. Possible intermediates are molecules found at the ends of microtubules such as the adenomatous polyposis coli gene product (Nathke et al., 1996), on microtubules such as mitogen-activated protein kinase (Morishima and Kosik, 1996), or calmodulin, which can affect the interaction of MAP2 and tau with actin (Kotani et al., 1985). The very complex array of MAP phosphorylation states, known to have an effect on microtubule dynamics (Drechsel et al., 1992) may also serve to regulate interactions with actin.

We thank Elizabeth Ackerman, Maura Schutt, and Cailin Monahan for technical assistance, Dr. Thomas Stossel for a critical reading of the manuscript, and Dr. Craig Garner for the generous gift of rat MAP2c cDNA.

This work was supported by National Institutes of Health grants CA57479, DK38452, and HL48743 (C.C. Cunningham), AR38910 (P.A. Janmey), and NS29031 and AG06601 (Kenneth S. Kosik). N. Leclerc acknowledges a Canadian Medical Research Council Fellowship.

Received for publication 6 February 1996 and in revised form 4 November 1996.

References

Almdal, K., J. Dyre, S. Hvidt, and O. Kramer. 1993. Towards a phenomenological definition of the term 'gel.' *Polymer Gels and Networks.* 1:5–17.

Asai, D.J., W.C. Thompson, L. Wilson, C.F. Dresden, H. Schulman, and D.L. Purich. 1985. Microtubule-associated proteins (MAPs): a monoclonal antibody to MAP 1 decorates microtubules *in vitro* but stains stress fibers and not microtubules *in vivo. Proc. Natl. Acad. Sci. USA.* 82:1434–1438.

Baas, P.W., T.P. Pienkowski, and K.S. Kosik. 1991. Processes induced by tau expression in Sf9 cells have an axon-like microtubule organization. *J. Cell Biol.* 115:1333–1344.

Baorto, D.M., W. Mellado, and M.L. Shelanski. 1992. Astrocyte process growth induction by actin breakdown. *J. Cell Biol.* 117:357–367.

Binder, L.I., A. Frankfurter, and L.I. Rebhun. 1986. Differential localization of MAP2 and tau in mammalian neurons in situ. *Proc. Natl. Acad. Sci. USA.* 81: 145–166.

Birgbauer, E., J.H. Dinsmore, B. Winckler, A.D. Lander, and F. Solomon. 1991. Association of ezrin isoforms with the neuronal cytoskeleton. *J. Neurosci. Res.* 30:232–241.

Brotschi, E.A., J.H. Hartwig, and T.P. Stossel. 1978. The gelation of actin by actin-binding protein. *J. Biol. Chem.* 253:8988–8993.

Caceres, A., and K.S. Kosik. 1990. Inhibition of neurite polarity by tau antisense oligonucleotides in primary cerebellar neurons. *Nature (Lond.).* 343: 461–463.

Caceres, A., S. Potrebic, and K.S. Kosik. 1991. The effect of tau antisense oligonucleotides on neurite formation of cultured cerebellar macroneurons. *J. Neurosci.* 11:1515–1523.

Caceres, A., J. Mautino, and K.S. Kosik. 1992. Suppression of MAP2 in cultured cerebellar macroneurons inhibits minor neurite formation. *Neuron.* 9: 607–618.

Chen, J., Y. Kanai, N.J. Cowan, and N. Hirokawa. 1992. Projection domains of MAP2 and tau determine spacings between microtubules in dendrites and axons. *Nature (Lond.).* 360:674–677.

Cooper, J.A., J. Bryan, B.D. Schwab, C. Frieden, D.J. Loftus, and E.L. Elson. 1987. Microinjection of gelsolin into living cells. *J. Cell Biol.* 104:491–501.

Correas, I., R. Padilla, and J. Avila. 1990. The tubulin-binding sequence of brain microtubule-associated proteins, tau and MAP-2, is also involved in actin binding. *Biochem. J.* 269:61–64.

Cross, D., C. Vial, and R.B. Maccioni. 1993. A tau-like protein interacts with stress fibers and microtubules in human and rodent cultured cell lines. *J. Cell Sci.* 105:51–60.

Cunningham, C. 1995. Actin polymerization and intracellular solvent flow in cell surface blebbing. *J. Cell Biol.* 129:1589–1599.

Cunningham, C.C., J.B. Gorlin, D.J. Kwiatkowski, J.H. Hartwig, P.J. Janmey, H.R. Byers, and T.P. Stossel. 1992. Actin-binding protein requirement for cortical stability and efficient locomotion. *Science (Wash. DC).* 255:325–327.

Dentler, W.L., and C. Adams. 1992. Flagellar microtubule dynamics in Chlamydomonas: cytochalasin D induces periods of microtubule shortening and elongation; and colchicine induces disassembly of the distal, but not proximal, half of the flagellum. *J. Cell Biol.* 117:1289–1298.

Drechsel, D.N., A.A. Hyman, M.H. Cobb, and M.W. Kirschner. 1992. Modulation of the dynamic instability of tubulin assembly by the microtubule-associated tau. *Mol. Biol. Cell.* 3:1141–1154.

Edson, K., B. Weisshaar, and A. Matus. 1993. Actin depolymerisation induces process formation on MAP2-transfected non-neuronal cells. *Development (Camb.).* 117:689–700.

Ferreira, A., R. Kincaid, and K.S. Kosik. 1993. Calcineurin is associated with the cytoskeleton of cultured neurons and has a role in the acquisition of polarity. *Mol. Biol. Cell.* 4:1225–1238.

Flory, P.J. 1953. Principles of Polymer Chemistry. Cornell University Press, Ithaca, NY. 672. pp.

Forscher, P., and S.J. Smith. 1988. Actions of cytochalasins on the organization of actin filaments and microtubules in a neuronal growth cone. *J. Cell Biol.* 107:1505–1516.

Fung, M.C., K.Y. Chiu, T. Weber, T.W. Chang, and N.T. Chang. 1988. Detection and purification of a recombinant human B lymphotropic virus (HHV-6) in the baculovirus expression system by limiting dilution and DNA dot-blot hybridization. *J. Virol. Methods.* 19:33–42.

Garner, C.C., and A. Matus 1988. Different forms of microtubule-associated protein 2 are encoded by separate mRNA transcripts. *J. Cell Biol.* 106:779–783.

Griffith, L.M., and T.D. Pollard. 1978. Evidence for actin filament-microtubule interaction mediated by microtubule-associated proteins. *J. Cell Biol.* 78: 958–965.

Griffith, L.M., and T.D. Pollard. 1982. The interaction of actin filaments with microtubules and microtubule-associated proteins. *J. Biol. Chem.* 257:9143–9151.

Hartwig, J.H., and P. Shevlin. 1986. The architecture of actin filaments and the ultrastructural location of actin-binding protein in the periphery of lung macrophages. *J Cell Biol.* 103:1007–1020.

Hartwig, J., M. Thelen, A. Rosen, P. Janmey, A. Nairn, and A. Aderem. 1992. The MARCKS protein is an actin filament crosslinking protein regulated by protein kinase C-mediated phosphorylation and by calcium/calmodulin. *Nature (Lond.).* 356:618–622.

Janmey, P.A. 1991. A torsion pendulum for measurement of the viscoelasticity of biopolymers and its application to actin networks. *J. Biochem. Biophys. Methods.* 22:41–53.

Janmey, P.A., S. Hvidt, J. Peetermans, J. Lamb, J.D. Ferry, and T.P. Stossel. 1988. Viscoelasticity of F-actin and F-actin/gelsolin complexes. *Biochemistry.* 27:8218–8227.

Janmey, P.A., S. Hvidt, J. Lamb, and T.P. Stossel. 1990. Resemblance of actin-binding protein/actin gels to covalently crosslinked networks. *Nature (Lond.).* 345:89–92.

Kindler, S., B. Schulz, M. Goedert, and C.C. Garner. 1990. Molecular structure of microtubule-associated protein 2b and 2c from rat brain. *J. Biol. Chem.* 265:19679–19684.

Kitts, P.A., M.D. Ayres, and R.D. Possee. 1990. Linearization of baculovirus DNA enhances the recovery of recombinant virus expression vectors. *Nucl. Acids Res.* 18:5667–5672.

Knops, J., K.S. Kosik, G. Lee, J.D. Pardee, G.L. Cohen, and L. McConlogue. 1991. Overexpression of tau in a nonneuronal cell induces long cellular processes. *J. Cell Biol.* 114:725–733.

Knowles, R., N. Leclerc, and K.S. Kosik. 1994. Organization of actin and microtubules during process formation in tau-expressing Sf9 cells. *Cell Motil. Cytoskel.* 28:256–264.

Kosik, K.S., L.D. Orecchio, L. Binder, J.Q. Trojanowski, V.M.-Y. Lee, and G. Lee. 1988. Epitopes that span the tau molecule are shared with paired helical filaments. *Neuron.* 1:817–825.

Kotani, S., E. Nishida, H. Kumagai, and H. Sakai. 1985. Calmodulin inhibits interaction of actin with MAP2 and tau, two major microtubule-associated proteins. *J. Biol. Chem.* 260:10779–10783.

Leclerc, N., P.W. Baas, C.C. Garner, and K.S. Kosik. 1996. Juvenile and mature MAP2 isoforms induce distinct patterns of process outgrowth. *Mol. Biol. Cell.* 7:443–455.

Lin, C-H., and P. Forscher. 1993. Cytoskeletal remodeling during growth cone-target interactions. *J. Cell Biol.* 121:1369–1383.

Lo, S.H., P.A. Janmey, J.H. Hartwig, and L.B. Chen. 1994. Interactions of tensin with actin and identification of its three distinct actin-binding domains. *J. Cell Biol.* 125:1067–1075.

McLaughlin, P.J., and A.G. Weeds. 1995. Actin-binding protein complexes at atomic resolution. *Annu. Rev. Biophys. Biomol. Struct.* 24:643–675.

Moraga, D.M., P. Nunez, J. Garrido, and R.B. Maccioni. 1993. A tau fragment containing a repetitive sequence induces bundling of actin filaments. *J. Neurochem.* 61:979–986.

Morishima, M., and K.S. Kosik. 1996. The pool of MAP kinase associated with

microtubules is small but constitutively active. *Mol. Biol. Cell.* 7:893–905.
Nathke, I.S., C.L. Adams, P. Polakis, J.H. Selin, and W.J. Nelson. 1996. The adenomatous polyposis coli tumor suppressor protein localizes to plasma membrane sites involved in active cell migration. *J. Cell Biol.* 134:165–179.
Nishida, E., T. Kuwaki, and H. Sakai. 1981. Phosphorylation of microtubule-associated proteins (MAPs) and pH of the medium control interaction between MAPs and actin filaments. *J. Biochem. (Tokyo).* 90:575–578.
Panda, D., J.E. Daijo, M.A. Jordan, and L. Wilson. 1995. Kinetic stabilization of microtubule dynamics at steady state *in vitro* by substoichiometric concentrations of tubulin-colchicine complex. *Biochemistry.* 34:9921–9929.
Papandrikopoulou, A., T. Doll, R.P. Tucker, C.C. Garner, and A. Matus. 1989. Embryonic MAP2 lacks the cross-linking sidearm sequences and dendritic targeting signal of adult MAP2. *Nature (Lond.).* 340:650–652.
Pollard, T.D. 1982. A falling ball apparatus to measure filament cross-linking. *Methods Cell Biol.* 24:301–311.
Pollard, T.D., S.C. Selden, and P. Maupin. 1984. Interaction of actin filaments with microtubules. *J. Cell Biol.* 99:33s–37s.
Rochlin, M.W., K.M. Wickline, and P.C. Bridgman. 1996. Microtubule stability decreases axon elongation but not axoplasm production. *J. Neurosci.* 16: 3236–3246.
Sanchez, I., and W.D. Cohen. 1994. Assembly and bundling of marginal band microtubule protein: role of tau. *Cell Motil. Cytoskel.* 29:57–71.
Satillaro, R.F. 1986. Interaction of microtubule-associated protein 2 with actin filaments. *Biochemistry.* 25:2003–2009.
Satillaro, R.F., W.L. Dentler, and E.L. LeCluyse. 1981. Microtubule-associated proteins (MAPs) and the organization of actin filaments in vitro. *J. Cell Biol.* 90:467–473.
Selden, S.C., and T.D. Pollard. 1986. Interaction of actin filaments with microtubules is mediated by microtubule-associated proteins and regulated by phosphorylation. *Ann. NY Acad. Sci.* 466:803–812.
Stossel, T.P. 1993. On the crawling of animal cells. *Science (Wash. DC).* 260: 1086–1094.
Tanaka, E., and J. Sabry. 1995. Making the connection: cytoskeletal rearrangements during growth cone guidance. *Cell.* 83:171–176.
Tanaka, E., T. Ho, and M.W. Kirschner. 1995. The role of microtubule dynamics in growth cone mobility and axonal growth. *J. Cell Biol.* 128:139–155.
Toso, R.J., M.A. Jordan, K.W. Farrell, B. Matsumoto, and L. Wilson. 1993. Kinetic stabilization of microtubule dynamic instability *in vitro* by vinblastine. *Biochemistry.* 32:1285–1293.
Umeyama, T., S. Okabe, Y. Kanai, and N. Hirokawa. 1993. Dynamics of microtubules bundled by microtubule-associated protein 2C (MAP2C). *J. Cell Biol.* 120:451–465.
Waterman-Storer, C.M., S. Karki, and E.L. Holzbaur. 1995. The p150Glued component of the dynactin complex binds to both microtubules and the actin-related protein centractin (Arp-1). *Proc. Natl. Acad. Sci. USA.* 92:1634–1638.
Watts, R.G., and T.H. Howard. 1994. Role of tropomyosin, α-actinin, and actin binding protein 280 in stabilizing Triton insoluble F-actin in basal and chemotactic factor activated neutrophils. *Cell Motil. Cytoskel.* 28:155–164.
Way, M., B. Pope, and A.G. Weeds. 1992. Evidence for functional homology in the F-actin binding domains of gelsolin and α-actinin: implications for the requirements of severing and capping. *J. Cell Biol.* 119:835–842.
Wille, H., E.-M. Mandelkow, J. Dingus, R.B. Vallee, L.I. Binder, and E. Mandelkow. 1992*a.* Domain structure and antiparallel dimers of microtubule-associated protein 2 (MAP2). *J. Struct. Biol.* 108:49–61.
Wille, H., E.-M. Mandelkow, and E. Mandelkow. 1992*b.* The juvenile microtubule-associated protein MAP2c is a rod-like molecule that forms antiparallel dimers. *J. Biol Chem.* 267:10737–10742.
Winkler, B., and F. Solomon. 1991. A role for microtubule bundles in the morphogenesis of chicken erythrocytes. *Proc. Natl. Acad. Sci. USA.* 88:6033–6037.